Characterization of a simple gas expansion ion source for intense pulses of subthermal molecular ions

Lukas Berger[1], Florian Grussie[1], Felix Nuesslein[1], Oldřich Novotný[1], Aigars Znotins[1], Joffrey Fréreux[2], Xavier Urbain[2], and Holger Kreckel[1]*
[1] *Max-Planck-Institut für Kernphysik, Saupfercheckweg 1, 69117 Heidelberg, Germany and*
[2] *Institute of Condensed Matter and Nanosciences, Université Catholique de Louvain, Louvain-la-Neuve B-1348, Belgium*

(Dated: December 6, 2024)

We describe a simple gas expansion ion source based on static discharge voltages and a commercially available pulsed valve. The discharge is initiated by the gas pulse itself between two high voltage electrodes, without the need for fast voltage switches or complex timing schemes. The ion source very reliably produces intense bursts of molecular ions (with currents exceeding 100 μA during the pulse-on phase) with only minor pulse-to-pulse variations in intensity and pulse shape. We have characterized the internal energy of H_3^+ and N_2O^+ ions produced by the ion source, using dissociative charge exchange and laser photodissociation, respectively. We find that collisions in the expanding gas reduce the internal energy of the molecular ions to well below room temperature.

I. INTRODUCTION

For gas phase experiments with molecular beams, the preparation and characterization of the internal excitation of the molecules is of paramount importance. It is well known that reaction rates can differ dramatically, depending on the vibrational and/or rotational states that are populated in the reacting molecules. Various techniques have been developed to control and diagnose the internal excitations for molecular beam experiments [1].

A very common method to reduce the temperatures of molecular beams is the employment of free jet expansions. This approach relies on the expansion of a gas from a high pressure reservoir (often several times higher than atmospheric pressure) into a vacuum vessel. If certain boundary conditions concerning the nozzle size and the mean free path of the gas in the reservoir are fulfilled, the process can be considered adiabatic and isentropic [2]. The adiabaticity condition will lead to the conservation of energy during the expansion, such that the sum of the kinetic energy and the enthalpy H are constant [3] along the direction of the mass flow (here denoted by the coordinate x)

$$\frac{1}{2}mv(x)^2 + H(x) = \text{const}, \tag{1}$$

where m stands for the mass of the molecules, and $v(x)$ is the velocity at position x. As a consequence, in an isentropic free jet expansion the local enthalpy (and thus the internal temperature) of the molecules in the expanding gas can be reduced dramatically, and converted into directed kinetic energy along the jet direction.

Very low internal temperatures can be realized for neutral molecules in uniform supersonic flows [4, 5]. Under ideal conditions, even extremely fragile species like the helium dimer molecule – a compound with a bond length of 50 Å and a binding energy of only 1.3 mK – can be produced and studied [6, 7].

From a technical point of view, it is often desirable to operate free jet expansions in pulsed mode instead of using continuous beams. Employing short gas pulses allows for a drastic reduction in the pumping requirements necessary to maintain the pressure gradient between the gas reservoir and the experimental vacuum chambers. Furthermore, if the gas pulse is short enough, interference due to molecules being reflected from the chamber walls can be ruled out. An early account of various efforts to create short gas pulses and their applications can be found in the review by Gentry [8]. Among the particular designs of fast valves that have become popular and seen much use in molecular beam experiments are the commercially available General Valve Series 9 [9], based on a plunger connected to a solenoid magnet, the high performance Even-Lavie valve [10, 11], which also makes use of a solenoid actuator, and the design of Proch and Trickl [12], which employs a piezo-electric flexing disc to retract the plunger.

Here, we report and characterize a simple supersonic expansion ion source that is based on the so-called *Amsterdam piezo valve* [13]. This type of valve also makes use of a piezo-actuator, but in the form of a cantilever instead of a flexing disc. The cantilever approach was originally pioneered by Gerlich [14], and in the meantime it has been optimized and commercialized. It is currently adopted by various groups around the world for a whole range of applications [15].

The use of a pulsed valve in an ion source is a somewhat more specialized application, and although a number of implementations of supersonic ion sources can be found in the literature, there is comparatively little quantitative information available on the internal temperatures that can be achieved. One has to keep in mind that the introduction of some sort of ionization process before the expansion usually goes along with a significant increase in the initial temperature of the molecules, which may

* holger.kreckel@mpi-hd.mpg.de

correspond to thousands of kelvin. In fact, the molecular ions may be created with a highly non-thermal distribution of internal states, and it is not obvious that full thermal equilibrium can be reached during the expansion process. Furthermore, since the ion density will always be much lower than the neutral density, detailed diagnostics of the populated individual ro-vibrational states are much more challenging for molecular ions.

Laperle et al. used an ion source based on the Proch and Trickl design to produce H_3^+ and D_3^+ ions for measurements of dissociative charge exchange [16]. The authors state that previous measurements with O_2^+ suggest rotational temperatures around 30 K, however, from the kinetic energy release spectra (following the neutralization of D_3^+ with caesium) they also infer that some vibrational excitation is probably still present. McCall et al. used a very similar ion source design to provide H_3^+ ions for storage ring measurements of dissociative recombination. Spectroscopic measurements were performed on the two lowest-lying rotational states of H_3^+ only, and from those populations temperatures between 20 and 60 K were inferred [17]. However, the lowest two states of H_3^+ belong to two different nuclear spin configurations, which will not be thermalized by collisions with an inert buffer gas. Deriving a temperature from their populations will probably probe the nuclear spin equilibrium upon production of the ions, rather than the rotational temperature. Therefore, these temperature values may be taken with a grain of salt.

Another set of measurements for H_3^+ ions with the same type of ion source were reported by Kreckel et al. [18]. This time, five rotational states were monitored using cavity ring-down spectroscopy, allowing for the determination of the rotational temperature of the ion samples. The measurements yielded 120 K for pure hydrogen discharges and 180 K for a 1:5 mixture of hydrogen and argon gas. In the same campaign a search for vibrational excitation produced negative results. In all of the studies mentioned above the flexing piezo-disc actuator design was used, and a discharge between two metallic electrodes close to the nozzle was triggered by a dedicated high voltage pulser.

A different approach has been used by the Neumark group to produce negative O_2^- ions [19] for slow electron velocity-map imaging studies. Here, a 1 keV electron beam is crossed with a supersonic expansion to produce cold anions. After photodetachment, the resulting O_2 is found to have a rotational temperature of 55 K, which is interpreted as an upper limit for the initial O_2^- ions. In a similar measurement with propynyl anions, the temperature of the ions is found to depend on the backing pressure (the results are compared to a 60 K simulation for the rotational degrees of freedom at medium pressure), while a certain amount of vibrational excitation (corresponding to a temperature of 230 K) is also found [20]. In a later publication from the same group, a supersonic ion source based on an Even-Lavie pulsed valve is described [21]. Here, the discharge takes place between a set of two grids, one of which is supplied with a static high voltage. The gas pulse therefore ignites the discharge by itself during the passage through the electrodes, without the need for a fast electronic switch to supply the discharge voltage. The authors use the ion source to produce nitrogen-doped carbon chain anions (C_2N^-, C_4N^-, C_6N^-), and they state that the grid discharge source produces internally colder ions than the other ion source implementations that were used previously. A similar grid ion source, but equipped with an *Amsterdam piezo valve*, is mentioned in a later publication of the same group [22].

Our expansion source design was inspired by the grid ion source described by the Neumark group, in particular by the use of a static high voltage supply. We have tried to simplify the set-up even further, by omitting the grids altogether and using two cylindrical discharge electrodes. This has the advantage that there is no obstruction in the discharge channel, and the plain electrodes are more robust than fine metal grids, which will be degraded by the harsh conditions in the discharge region over time.

Our group works with stored molecular ions in ion traps or storage rings. Our central facility is the Cryogenic Storage Ring (CSR) [23], a fully electrostatic and cryogenic storage device with a circumference of 35 m. Most infrared-active molecular ions stored inside the CSR at cryogenic temperatures will cool to their lowest rotational states by spontaneous emission of radiation [24–27]. However, there are a number of very fundamental molecular ions that will not cool radiatively, owing to the lack of a permanent dipole moment (e.g., H_2^+, O_2^+, H_3^+, etc ...). These ions will have to be cooled actively

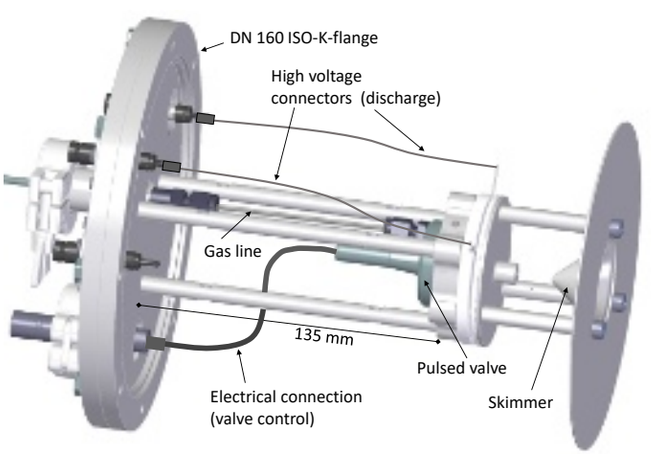

FIG. 1. Isometric view of the supersonic expansion ion source mounted on a standard ISO-K 160 flange. All connections are supplied through feed-throughs in the mounting flange. A skimmer with a surrounding disc fitting the inner tube diameter of the vacuum chamber is mounted downstream of the nozzle, in order to allow for efficient differential pumping if experimentally required.

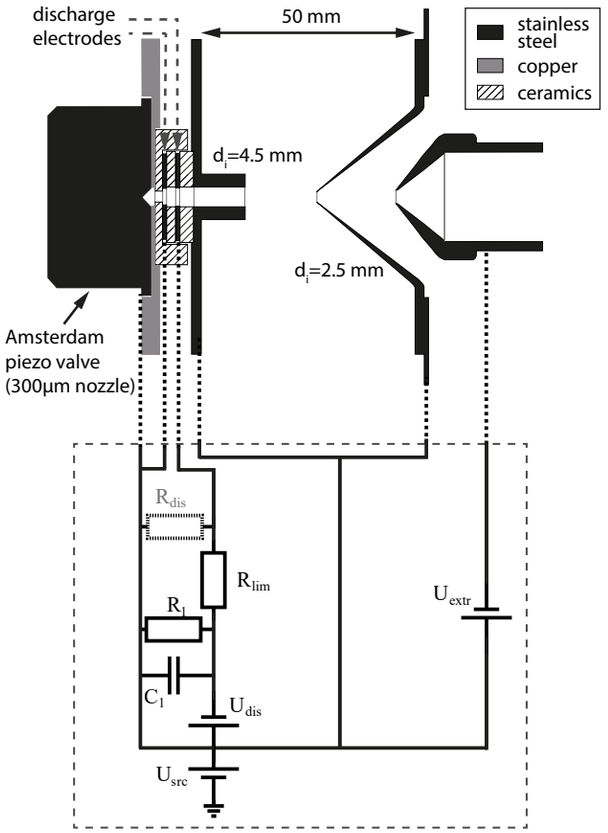

FIG. 2. Schematic of the discharge unit of the ion source. The two discharge electrodes are supplied with a static high voltage. A simple electric circuit is given below the drawing. It was designed to limit the discharge current and buffer the output of the high voltage power supply with a capacitor. This makes the operation of the source largely independent of the output resistance of the power supply. Typical values are: $R_{\rm lim} = 1.25\,{\rm k}\Omega$, $U_{\rm dis} = 0.7-2\,{\rm kV}$, $C_1 = 1\,\mu{\rm F}$, $R_1 = 5\,{\rm M}\Omega$ (the resistance $R_{\rm dis}$ is not a component of the electric circuit, it represents the finite resistance through the gas during the discharge-on phase). We used $U_{\rm extr} = 8\,{\rm kV}$ to extract the ions from the source region, while the total ion source potential $U_{\rm src}$ can be as high as 30 kV in our case.

prior to injection into the CSR, which was one of the main motivations for the present ion source design. For typical experiments at the CSR, it is beneficial to use intense pulses of molecular ions with the length of only a few tens of microseconds. In order to be able to fill the storage ring with a single pulse, the present source design has a rather large nozzle diameter to maximize the output. Moreover, it is crucial for the measurements that the ion source conditions are reproducible, stable on the timescale of a week of operation, and that shot-to-shot fluctuations are kept to a minimum. These aspects will be demonstrated and quantified in the present paper. While we have optimized the design of the ion source with the operation at ion traps or storage rings in mind, we believe that very similar parameters and requirements would apply if the ion source is employed at other facilities and experimental setups.

This manuscript is organized as follows: the next section describes the source design and operation. In Section III we report on charge exchange measurements with H_3^+ ions to characterize the internal excitation of the ions, and in Section IV photodissociation measurements with N_2O^+ ions are presented. In the final section we provide a summary and conclusions.

II. DESIGN AND OPERATION

At the CSR, we employ a wide variety of ion sources for positive and negative ions. To make the ion sources modular and facilitate exchange, we have developed certain standards for the connectors and dimensions that we try to adhere to. We typically use a three-way DN 160 ISO-K T-piece to house the ion source. This allows for efficient pumping of the chamber at the 90 degree port with a turbomolecular pump. We try to supply all the gas and all electrical connections through the mounting flange of the source, such that we can pull the entire source out without the need to open additional vacuum ports. Figure 1 shows an isometric view of the expansion ion source, including the mounting flange and the skimmer. We use a commercial pulsed *Amsterdam piezo valve* [13], with a relatively large nozzle diameter of 300 μm.

The skimmer is designed to sit on a disc whose diameter (152.5 mm) is only 0.5 mm smaller than the inner diameter of our DN160 ISO-K vacuum tube, such that the gas flow into the next chamber is restricted and efficient differential pumping is facilitated. The distance from the nozzle of the pulsed valve to the tip of the skimmer is 38 mm in our implementation. It should be noted, however, that for the designated use of the ion source, i.e., to produce ion pulses to be injected into an ion trap or storage ring, the exact skimmer design is less relevant (as long as the skimmer is properly centered). Since we often need only a single pulse every few seconds or minutes, gas build-up in the chamber and reflections from the chamber wall can be neglected. However, for the ion source characterization, it is often convenient to operate the source with a repetition rate of hundreds of hertz, and then an efficient differential pumping scheme becomes crucial, to keep the pressure in the adjacent chambers in an acceptable range.

The schematic of the discharge stack mounted on the front of the valve is shown in Fig. 2. The discharge is initiated by the gas pulse between the two round metal electrodes. We tested a preliminary design where the receptacle for the electrodes and the insulator discs were made from Polytetrafluoroethylene (PTFE). While the source performed well, we found that after a few days of operation (using only hydrogen and noble gases) higher voltages were needed to ignite the discharge. When dismantled, the PTFE insulators and parts of the metal elec-

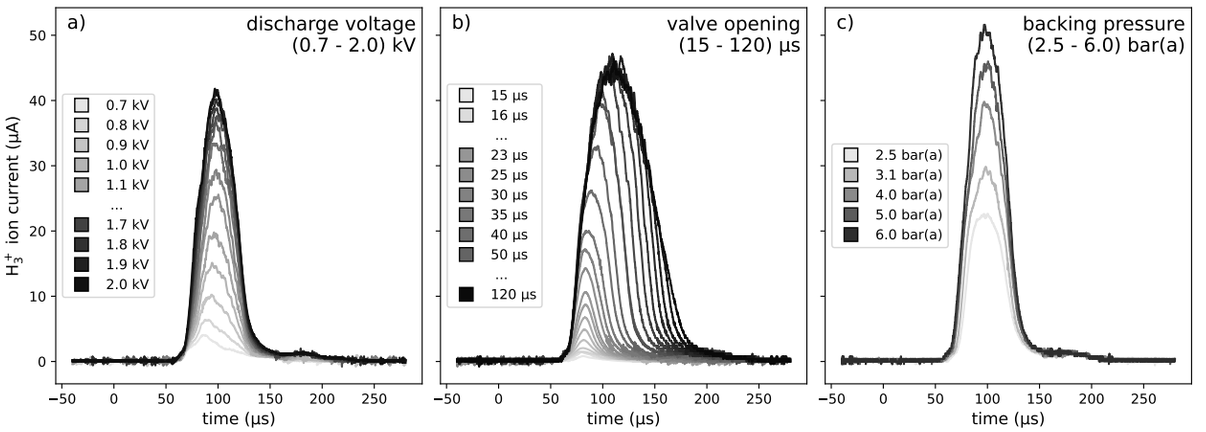

FIG. 3. The plots show the output pulses of H_3^+ ions, measured as an ion current for various ion source parameters. The H_3^+ ions were mass-selected by a dipole magnet, and the signals were recorded using a fast current amplifier attached to a Faraday cup. a) Variation of the discharge voltage between 0.7 and 2 kV (the darker grey colors signify increasing voltage), for a valve opening time of 50 μs, and a backing pressure of 4 bar(a). b) Variation of the valve opening time between 15 and 120 μs (darker grey colors signify longer opening times) for a discharge voltage of 1.9 kV and a backing pressure of 4 bar(a). c) Variation of the backing pressure between 2.5 and 6 bar(a) (darker grey colors signify higher pressure), for a valve opening time of 50 μs and a discharge voltage of 1.9 kV.

trodes were severely discolored, in particular around the discharge area. After cleaning the source, we replaced all PTFE parts with new ones made from Macor® (machinable glass ceramic), which has better heat-resistance. After this modification we were able to operate the source for weeks without changes in its characteristics.

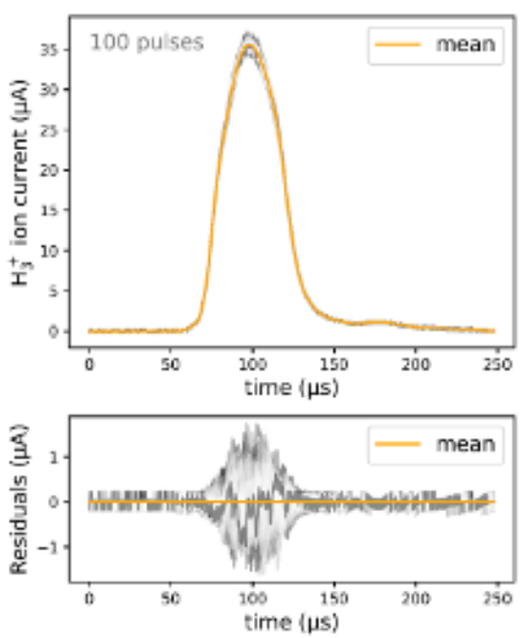

FIG. 4. Plot of a typical H_3^+ current signal, recorded as oscilloscope traces for 100 consecutive pulses. The mean value of all traces is plotted in yellow. The lower panel shows the residuals (the difference between the individual traces and the mean value) superimposed for all pulses, indicating a shot-to-shot variation at the current maximum of $< 3\%$.

Discharge voltages U_{dis} used for the operation with hydrogen range from 0.7 to 2 kV. While it is possible to connect the discharge electrodes directly to a high voltage power supply, we found that in this case the source performance will depend on the output resistance and capacitance of the power supply, and the pulse intensity may vary with the repetition rate. These output variations are probably owed to the regulation circuit of the power supply, which has to cope with the breakdown of the resistance (and the corresponding surge in the current) that occurs while the discharge is active. To mitigate this effect, and make the ion source performance largely independent of the choice of the high voltage power supply, we use a simple electric circuit that is shown in the lower part of Fig. 2. We recommend to buffer the discharge voltage with a high voltage capacitor (C_1 in Fig 2) and limit the discharge current with an ohmic resistance (R_{lim} in Fig 2). The resistor R_1 is introduced for safety reasons, to ensure that the capacitor will not remain charged for extended periods of time after the source has been used and the power supply is disconnected. We extract the ions from the source region with a negative potential of $U_{\mathrm{extr}} = 8$ kV, while the total potential U_{src} between ground and the source is used to accelerate the ions to a specific kinetic energy that we need for transfer from the high voltage platform to the CSR. This double-stage extraction scheme may not be needed for other applications.

To quantify the output of the ion source we measured the ion current in a Faraday cup, 5 m downstream of the ion source. The ions were mass-selected by a dipole magnet, and we used a fast current amplifier (FEMTO

DLPCA-200) with a rise time $< 1\,\mu$s to record the signal on a digital oscilloscope. We operated the source with a mixture of helium (80%) and hydrogen (20%) gas in order to create triatomic hydrogen ions H_3^+, which are produced in the well-known ion-neutral reaction

$$H_2^+ + H_2 \longrightarrow H_3^+ + H\,. \qquad (2)$$

This reaction is exothermic by 1.7 eV and very efficient. Therefore, H_3^+ always becomes the dominant ion in hydrogen discharges at higher pressure. Here, the helium is used as a buffer gas to produce lower internal temperatures, both by collisional de-excitation and via the reaction $H_2^+(v > 1) + He \longrightarrow HeH^+ + H$ [28].

Figure 3 shows the source output in the form of the H_3^+ current for various source conditions. We varied the discharge voltage between 0.7 and 2 kV, the valve opening time between 15 and 120 μs, and the backing pressure between 2.5 and 6 bar(a) (absolute pressure in units of bar). In all cases the source shows the expected behavior. The ion current increases steadily with the discharge voltage, the pulse opening time, and the backing pressure, while the shape of the pulses remains well-behaved, yielding peak currents of up to 50 μA. We also operated the ion source with pure hydrogen gas, in this case we observed H_3^+ ion currents exceeding 200 μA.

Figure 4 shows the accumulated oscilloscope traces for 100 consecutive pulses at constant ion source conditions (discharge voltage 1.9 kV, backing pressure 4.5 bar(a), valve opening time 50 μs), together with their averaged signal and the residuals. While the ion current reaches values around 35 μA, the pulse-to-pulse fluctuations at the maximum value are $< 3\,\%$. We observed a slow reduction of $< 5\,\%$ in intensity in the course of several hours of operation at 1 Hz, probably due to fluctuations in the backing pressure caused by the reducer at the gas bottle.

III. CHARGE EXCHANGE MEASUREMENTS WITH H_3^+ IONS

The triatomic hydrogen molecular ion H_3^+ is the simplest polyatomic molecule. In its ground state, it has the shape of an equilateral triangle, with three vibrational modes. The symmetric stretch mode ν_1 is infrared-inactive, while the two bending modes ν_2 are energetically degenerate (see [29] for details on quantum numbers and nomenclature). H_3^+ does not possess stable electronically excited states, and the neutral H_3 molecule is unstable.

Previous measurements of dissociative charge exchange between H_3^+ ions and alkali metal atoms (which effectively neutralize H_3^+ by electron donation) have shown that the internal energy of the H_3^+ molecules is transferred to the kinetic energy of its neutral fragments

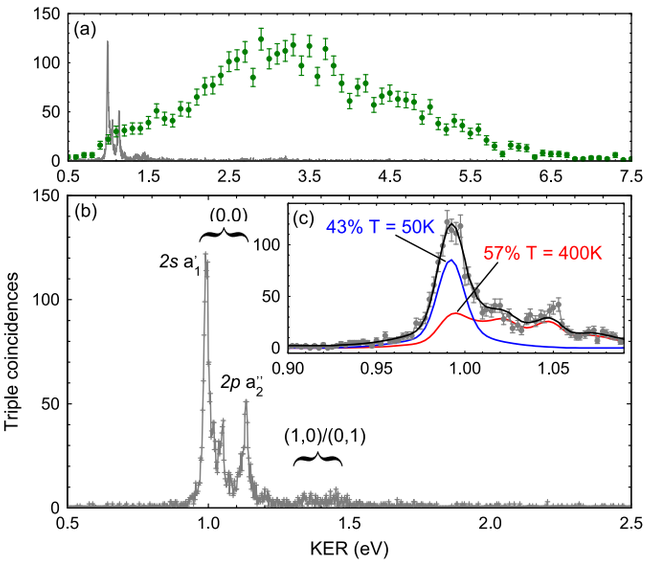

FIG. 5. Total kinetic energy release (KER) spectrum recorded for the three-body breakup of H_3^+ following dissociative charge exchange with potassium. (a) Qualitative comparison of a KER spectrum obtained using a standard discharge ion source (green markers) compared to a KER spectrum obtained with the expansion source (grey line). (b) KER spectrum obtained with the supersonic expansion source operated with a gas mixture of He:H_2 = 4:1. (c) Fit of the excess energy in the KER spectrum of the expansion source, interpreted as rotational excitation and represented by a bi-modal temperature distribution (see main text for details)

[16, 30]. The low ionization potential causes the low-lying $2s\,a_1'$ and $2p\,a_2''$ Rydberg states of H_3 to be populated. Their pre-dissociation leads to two- and three-body breakup. Determining the total kinetic energy release (KER) in the latter case informs on the internal energy of the intermediate Rydberg state, hence on that of the parent ion possessing the same overall geometry.

The present experiment was carried out at a dedicated setup located at the Université catholique de Louvain in Louvain-la-Neuve, Belgium. The H_3^+ ions were accelerated to 4 keV before encountering a potassium jet effusing from an oven through an array of capillaries. Fragments resulting from dissociative charge exchange were detected at the end of a 1.5 m long flight tube. Individual events were recorded using the multihit position- and time-sensitive detection system COBRA (COrrelation between BRightness and Amplitude), which has been described in a previous publication [31]. The detector consists of three stacked microchannel plates (Z-stack) that are backed with a phosphor screen. Light spots from the phosphor screen and electronic timing pulses from the microchannel plates are collected by a triggerable CMOS camera and a waveform digitizer, respectively. For the present measurements, triple hits were selected and analyzed, and a center-of-mass cut was applied to select true coincidence events.

Figure 5(a) shows a typical KER spectrum obtained using a standard discharge ion source. The very broad KER distribution reflects the unspecific internal excitation of the molecular ensemble, dispersed over hundreds of vibrational and rotational states. The situation changes dramatically for the KER spectrum obtained using the supersonic expansion source, shown in Figs. 5(b),(c). Here, two narrow peaks at ∼1 eV and ∼1.1 eV dominate the KER distribution, corresponding to $2s\,a_1'$ and $2p\,a_2''$ Rydberg states in their vibrational ground state, while a minor contribution (< 5%) of the first symmetric (1,0) and antisymmetric (0,1) stretch may be seen for both Rydberg states between ∼1.3 eV and ∼1.5 eV. This observation does not necessarily imply the same vibrational excitation is present in the parent ion, since the multidimensional Franck-Condon overlap is not fully diagonal. Rare events with a KER < 1 eV are probably caused by H_3 molecules in metastable states, which decay on their path to the detector.

The rotational excitation is visible in the KER spectrum of the expansion source as a shoulder toward higher energies, although not fully resolved in the present experiment (the energy resolution for the present data is on the order of ∼15 meV FWHM). By means of a simulation based on the H_3^+ line list [32] and the partition function, we achieved a very good fit using a bi-modal temperature distribution. The partial contributions and the total fit are plotted in Fig. 5(c). The fit result corresponds to an internal temperature of $T = (50 \pm 20)$ K for (43 ± 5)% of the ions, and a higher temperature of $T = (400 \pm 50)$ K for (57±4)%.

While these values may appear high when compared to temperatures of neutral species cooled in jet expansions, one has to keep in mind that the formation reaction (Eq. 2) produces H_3^+ with average internal energies exceeding 1 eV [33] (corresponding to ∼3300 K [34, 35]). Furthermore, H_3^+ features two different nuclear spin modifications that will not equilibrate in collisions with a noble buffer gas, and the level spacing of the lowest rotational states is large. Therefore, the present results indicate that about ∼25% and ∼30% of the H_3^+ ions are in the respective ortho and para ground states, while the higher temperature component is comprised of a dozen additional rotational states with rather small individual populations. This has to be contrasted with the nascent distribution, where the population would be spread out over more than a thousand states (H_3^+ has ∼700 states below 1 eV alone). The expansion source therefore yields ion ensembles that are much more concentrated in the lowest rotational states, which will prove very valuable for potential use in future spectroscopy experiments [36].

Furthermore, our results indicate that while rotational cooling is rather effective (as expected), vibrational cooling may not have reached the ground state for all ions. However, for the present applications the rotational cooling is much more important, as the vibrational lifetimes are short enough that the ground vibrational state will be reached within 2 s of storage in an ion trap or storage ring [37].

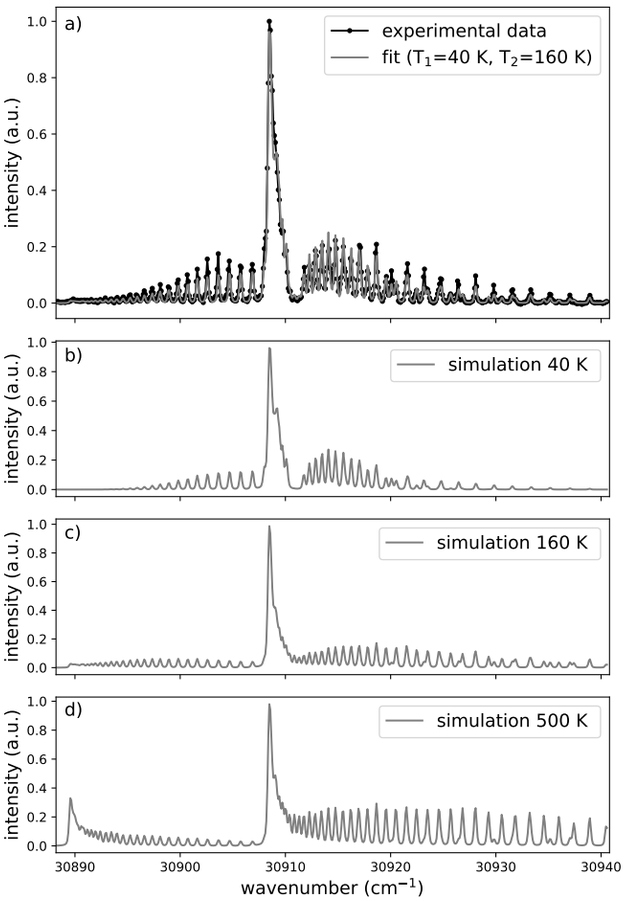

FIG. 6. Photodissociation signal of N_2O^+ ions exposed to a tunable pulsed dye laser, as a function of the laser frequency (in wavenumbers). a) Experimental signal (black markers) together with a fit (grey line) characterized by two temperatures. The fit indicates that 72% of the N_2O^+ ions have a rotational temperature of (40±10) K and 28% of the ions have a temperature of (160 ± 60) K. b),c),d) Simulated photodissociation signals for temperatures of 40 K, 160 K, and 500 K, respectively.

IV. PHOTODISSOCIATION OF THE NITROUS OXIDE CATION

As a second test case, we have studied the internal excitation of N_2O^+ ions produced in the expansion source. To this end we have used photodissociation spectroscopy of N_2O^+, employing the STARGATE setup (Spectroscopy of Transient Anions and Radicals by Gated and Accelerated Time-of-flight Experiment) at the Université catholique de Louvain in Louvain-la-Neuve, Belgium. The experimental setup was described in detail in a previous publication [38], here we will outline only the major features. The STARGATE setup uses

two mass-selecting stages to first pre-select the ions of interest, which are subsequently dissociated by a pulsed laser, and the second stage is used to select charged photo-fragmentation products. The first stage is accomplished by a gating, bunching and re-referencing cell, which, in conjunction with a pulsed deflector, serves as a time-of-flight mass-selector to create pulses of N_2O^+ ions and discriminate against other unwanted species. The N_2O^+ ions are exposed to a pulsed dye laser (Continuum ND6000, operating at 30 Hz, with 0.6 mJ per pulse and 5 ns pulse length), which will dissociate a fraction of them. Positively charged fragments are selected by a cylindrical electrostatic energy analyzer [39] and recorded by a microchannel plate detector.

The photodissociation of N_2O^+ has been studied extensively in the past [40–47], and it has been used recently to follow the internal cooling of N_2O^+ ions inside a cryogenic storage ring [48]. We focused on the following two-step pre-dissociation process

$$N_2O^+(\tilde{X}^2\Pi(000)) \xrightarrow{\text{excit.}} N_2O^+(\tilde{A}^2\Sigma^+(002)), \quad (3)$$

$$\xrightarrow{\text{diss.}} NO^+(\tilde{X}^1\Sigma^+) + N(^4S), \quad (4)$$

which required the laser to be operated between 323 and 324 nm, while the energy-analyzer was adjusted to select the NO^+ fragments. Based on previous measurements, the molecular parameters of all levels are known with high precision. In fact, the parameters of the upper $\tilde{A}^2\Sigma^+(002)$ level have recently been revised based on high resolution measurements carried out with the STARGATE setup [38]. Furthermore, in the same study a PGOPHER [49] profile for the relevant states of N_2O^+ was created, allowing for a detailed rovibrationally-resolved simulation of the photodissociation signal at various temperatures. We will make use of this code to benchmark the rotational temperature produced by our ion source.

For our tests, we chose typical operating conditions with a mixture of 93% argon and 7% N_2O at a total pressure of 3 bar(a). The valve opening time was set to 28 μs and the discharge voltage was kept at 1000 V.

Figure 6 shows the experimental photodissociation signal (relative intensity of the NO^+ signal) as a function of the frequency of the pulsed dye laser. The frequency has been calibrated and normalized to the strong peak at $\sim$30907 cm^{-1}. Also shown are the PGOPHER simulations of the photodissociation signal at three different temperatures. Fitting a range of temperatures to the experimental spectrum revealed that none of the simulated curves using a single temperature is sufficient to provide a good fit to the measured data. The majority of the experimental signal appears compatible with a temperature of 37 K. However, the existence of features at photon energies exceeding 30920 cm^{-1} and a very small feature at 30890 cm^{-1} indicate that a fraction of the ions possess a higher degree of internal excitation. We achieved the best fit assuming that (72 ± 2)% of the ions have a rotational temperature of $T = (40 \pm 10)$ K and (28 ± 2)% of the ions have a temperature of $T = (160 \pm 60)$ K. The corresponding simulated photodissociation signal is depicted by the grey line in Fig. 6(a). Combining more than two temperatures did not improve the quality of the fit.

Our results indicate that the ions are cooled significantly in the supersonic expansion ion source, compared with other ion sources. For example, previous studies at the RICE storage ring found a rotational temperature of 320 K for N_2O^+ ions produced in an electron cyclotron resonance (ECR) ion source [48]. This temperature remained essentially unchanged even after 200 s of storage in the cryogenic vacuum of the storage ring, owing to the small permanent dipole moment of the molecule. It should be noted that in our study, we do not probe vibrationally excited states, as in our experiments with stored ions, vibrationally excited states of molecules with comparatively low symmetry usually decay within the first few seconds of storage. For example, in the study of Hirota [48] et al., up to 10% of the N_2O^+ ions (created in an ECR ion source) were found to be vibrationally excited after 1 s of storage, but this value dropped to less than 1% after 5 s.

V. SUMMARY AND CONCLUSION

We have described and characterized a simple supersonic expansion ion source with static discharge voltages. The source reliably produces very strong pulses of small molecular ions with minimal pulse-to-pulse variations, which renders it an ideal and very compact source of ion bunches for applications with ion storage devices. Since the source is based on a commercial valve and a very basic electric circuit, it should be easy to replicate.

We have used the source to produce H_3^+ and N_2O^+ ions and study their internal temperatures by means of dissociative charge transfer and laser photodissociation, respectively.

For H_3^+, we found a bi-modal KER distribution, with 43% of the ions represented by an internal temperature of 50 K and 57% at a temperature of 400 K. Our measurements show a marked difference compared to results obtained with a standard discharge ion source, where the KER shows a broad distribution with no distinctive features. Detailed analysis of the expansion source spectrum indicates that more than 50% of the H_3^+ ions are in the combined ortho and para ground states.

In photodissociation studies with N_2O^+ ions, we obtained qualitatively similar results. Here, 72% of the ions were found to have a rotational temperature of 40 K, while 28% have a temperature of 160 K. Again, the expansion source clearly produces much colder ions than standard ion sources, while the origin of the bi-modal distribution is presently unclear.

Considering the fact that N_2O^+ is produced by direct ionisation of N_2O, while H_3^+ is produced by ionization of H_2 followed by proton transfer, the similarity in the results suggests the general applicability of the present

source design. It should be noted that the ion source setup described here was optimized for strong ion pulses. Therefore we chose a rather large and straight nozzle. There is certainly potential for further tests with different nozzle and extraction geometries to achieve lower temperatures, possibly at the expense of the pulse intensities.

ACKNOWLEDGMENTS

This work was supported by the Max Planck Society. X.U. is a Senior Research Associate of the Fonds de la Recherche Scientifique - FNRS, and acknowledges support under grant No. 4.4504.10. J.F. acknowledges the financial support provided by the Fédération Wallonie Bruxelles, through the project "iBEAM" funded by its research program "Actions de Recherche Concertées" (grant No. 18/23-090) and the Fonds de la Recherche Scientifique for a "mandat d'impulsion scientifique" (MIS, grant No. F.4038.24).

[1] R. Campargue, ed., Atomic and molecular beams: The state of the art 2000 (Springer, Berlin,. Heidelberg, 2001).
[2] M. D. Morse, Supersonic beam sources, in *Atomic, Molecular, and Optical Physics: Atoms and Molecules*, Experimental Methods in the Physical Sciences, Vol. 29, edited by F. Dunning and R. G. Hulet (Academic Press, 1996) pp. 21–47.
[3] H. Liepmann and A. Roshko, *Elements of gasdynamics* (John Wiley & Sons Inc., New York, London, Sydney, 1957).
[4] B. R. Rowe, G. Dupeyrat, J. B. Marquette, D. Smith, N. G. Adams, and E. E. Ferguson, The reaction O_2^++CH_4→$CH_3O_2^+$+H studied from 20 to 560 K in a supersonic jet and in a SIFT, J. Chem. Phys. **80**, 241 (1984).
[5] I. W. M. Smith, Reactions at very low temperatures: Gas kinetics at a new frontier, Angew. Chem. Int. Ed. **45**, 2842 (2006).
[6] F. Luo, G. C. McBane, G. Kim, C. F. Giese, and W. R. Gentry, The weakest bond: Experimental observation of helium dimer, J. Chem. Phys. **98**, 3564 (1993).
[7] W. Schollkopf and J. P. Toennies, Nondestructive Mass Selection of Small van der Waals Clusters, Science **266**, 1345 (1994).
[8] W. Gentry, Chapt. 3, in *Atomic and Molecular Beam methods*, edited by G. Scoles (Oxford University Press, Oxford, 1989).
[9] L. Abad, D. Bermejo, V. J. Herrero, J. Santos, and I. Tanarro, Performance of a solenoid-driven pulsed molecular-beam source, Rev. Sci. Instrum. **66**, 3826 (1995).
[10] U. Even, J. Jortner, D. Noy, N. Lavie, and C. Cossart-Magos, Cooling of large molecules below 1 K and He clusters formation, J. Chem. Phys. **112**, 8068 (2000).
[11] U. Even, The Even-Lavie valve as a source for high intensity supersonic beam, EPJ Techn. Instrum. **2**, 17 (2015).
[12] D. Proch and T. Trickl, A high-intensity multi-purpose piezoelectric pulsed molecular beam source, Rev. Sci. Instrum. **60**, 713 (1989).
[13] D. Irimia, D. Dobrikov, R. Kortekaas, H. Voet, D. A. van den Ende, W. A. Groen, and M. H. M. Janssen, A short pulse (7 μs FWHM) and high repetition rate (dc-5kHz) cantilever piezovalve for pulsed atomic and molecular beams, Rev. Sci. Instrum. **80**, 113303-113303-6 (2009).
[14] D. Gerlich, G. Jerke, U. Muck, and U. Person, Internal technical document, Freiburg University, *Schnelles Ventil zur Erzeugung sehr kurzer Gasimpulse* (1990).
[15] Website MassSpecpecD BV, Enschede, The Netherlands: https://www.amsterdampiezovalve.com/home.
[16] C. M. Laperle, J. E. Mann, T. G. Clements, and R. E. Continetti, Three-Body Dissociation Dynamics of the Low-Lying Rydberg States of H_3 and D_3, Phys. Rev. Lett. **93**, 153202 (2004).
[17] B. J. McCall, A. J. Huneycutt, R. J. Saykally, N. Djuric, G. H. Dunn, J. Semaniak, O. Novotny, A. Al-Khalili, A. Ehlerding, F. Hellberg, S. Kalhori, A. Neau, R. D. Thomas, A. Paal, F. Österdahl, and M. Larsson, Dissociative recombination of rotationally cold $H^+{}_3$, Phys. Rev. A **70**, 052716 (2004).
[18] H. Kreckel, O. Novotný, K. N. Crabtree, H. Buhr, A. Petrignani, B. A. Tom, R. D. Thomas, M. H. Berg, D. Bing, M. Grieser, C. Krantz, M. Lestinsky, M. B. Mendes, C. Nordhorn, R. Repnow, J. Stützel, A. Wolf, and B. J. McCall, High-resolution storage-ring measurements of the dissociative recombination of $H_3{}^+$ using a supersonic expansion ion source, Phys. Rev. A **82**, 042715 (2010).
[19] D. J. Leahy, D. L. Osborn, D. R. Cyr, and D. M. Neumark, Predissociation dynamics of the O_2 $B^3\Sigma_u^-$ state: Vibrational state dependence of the product fine-structure distribution, J. Chem. Phys. **103**, 2495 (1995).
[20] J. Zhou, E. Garand, W. Eisfeld, and D. M. Neumark, Slow electron velocity-map imaging spectroscopy of the 1-propynyl radical, J. Chem. Phys. **127**, 034304 (2007).
[21] E. Garand, T. I. Yacovitch, and D. M. Neumark, Slow photoelectron velocity-map imaging spectroscopy of C_2N^-, C_4N^-, and C_6N^-, J. Chem. Phys. **130**, 064304 (2009).
[22] B. Nichols, E. N. Sullivan, M. Ryazanov, C. M. Hong, and D. M. Neumark, Investigation of the two- and three-fragment photodissociation of the tert-butyl peroxy radical at 248 nm, J. Chem. Phys. **147**, 134304 (2017).
[23] R. von Hahn, A. Becker, F. Berg, K. Blaum, C. Breitenfeldt, H. Fadil, F. Fellenberger, M. Froese, S. George, J. Göck, M. Grieser, F. Grussie, E. A. Guerin, O. Heber, P. Herwig, J. Karthein, C. Krantz, H. Kreckel, M. Lange, F. Laux, S. Lohmann, S. Menk, C. Meyer, P. M. Mishra, O. Novotný, A. P. O'Connor, D. A. Orlov, M. L. Rappaport, R. Repnow, S. Saurabh, S. Schippers, C. D. Schröter, D. Schwalm, L. Schweikhard, T. Sieber, A. Shornikov, K. Spruck, S. Sunil Kumar, J. Ullrich,

X. Urbain, S. Vogel, P. Wilhelm, A. Wolf, and D. Zajfman, The cryogenic storage ring CSR, Rev. Sci. Instrum. **87**, 063115 (2016).

[24] A. P. O'Connor, A. Becker, K. Blaum, C. Breitenfeldt, S. George, J. Göck, M. Grieser, F. Grussie, E. A. Guerin, R. von Hahn, U. Hechtfischer, P. Herwig, J. Karthein, C. Krantz, H. Kreckel, S. Lohmann, C. Meyer, P. M. Mishra, O. Novotný, R. Repnow, S. Saurabh, D. Schwalm, K. Spruck, S. Sunil Kumar, S. Vogel, and A. Wolf, Photodissociation of an Internally Cold Beam of CH^+ Ions in a Cryogenic Storage Ring, Phys. Rev. Lett. **116**, 113002 (2016).

[25] C. Meyer, A. Becker, K. Blaum, C. Breitenfeldt, S. George, J. Göck, M. Grieser, F. Grussie, E. A. Guerin, R. von Hahn, P. Herwig, C. Krantz, H. Kreckel, J. Lion, S. Lohmann, P. M. Mishra, O. Novotný, A. P. O'Connor, R. Repnow, S. Saurabh, D. Schwalm, L. Schweikhard, K. Spruck, S. Sunil Kumar, S. Vogel, and A. Wolf, Radiative Rotational Lifetimes and State-Resolved Relative Detachment Cross Sections from Photodetachment Thermometry of Molecular Anions in a Cryogenic Storage Ring, Phys. Rev. Lett. **119**, 023202 (2017).

[26] O. Novotný, P. Wilhelm, D. Paul, Á. Kálosi, S. Saurabh, A. Becker, K. Blaum, S. George, J. Göck, M. Grieser, F. Grussie, R. von Hahn, C. Krantz, H. Kreckel, C. Meyer, P. M. Mishra, D. Muell, F. Nuesslein, D. A. Orlov, M. Rimmler, V. C. Schmidt, A. Shornikov, A. S. Terekhov, S. Vogel, D. Zajfman, and A. Wolf, Quantum-state-selective electron recombination studies suggest enhanced abundance of primordial HeH^+, Science **365**, 676 (2019).

[27] Á. Kálosi, M. Grieser, R. von Hahn, U. Hechtfischer, C. Krantz, H. Kreckel, D. Müll, D. Paul, D. W. Savin, P. Wilhelm, A. Wolf, and O. Novotný, Laser Probing of the Rotational Cooling of Molecular Ions by Electron Collisions, Phys. Rev. Lett. **128**, 183402 (2022).

[28] X. N. Tang, H. Xu, T. Zhang, Y. Hou, C. Chang, C. Y. Ng, Y. Chiu, R. A. Dressler, and D. J. Levandier, A pulsed-field ionization photoelectron secondary ion coincidence study of the $H_2^+(X, v^+ = 0-15, N^+ = 1)$+He proton transfer reaction, J. Chem. Phys. **122**, 164301 (2005).

[29] C. Lindsay and B. J. McCall, Comprehensive Evaluation and Compilation of H_3^+ Spectroscopy, J. Mol. Spectr. **210**, 60 (2001).

[30] U. Galster, F. Baumgartner, U. Müller, H. Helm, and M. Jungen, Experimental and quantum-chemical studies on the three-particle fragmentation of neutral triatomic hydrogen, Phys. Rev. A **72**, 062506 (2005).

[31] X. Urbain, D. Bech, J.-P. Van Roy, M. Géléoc, S. J. Weber, A. Huetz, and Y. J. Picard, A zero dead-time multi-particle time and position sensitive detector based on correlation between brightness and amplitude, Rev. Sci. Instrum. **86**, 023305 (2015).

[32] I. I. Mizus, A. Alijah, N. F. Zobov, L. Lodi, A. A. Kyuberis, S. N. Yurchenko, J. Tennyson, and O. L. Polyansky, ExoMol molecular line lists – XX. A comprehensive line list for H_3^+, Mon. Not. R. Astron. Soc. **468**, 1717 (2017).

[33] K. Höveler, J. Deiglmayr, J. A. Agner, H. Schmutz, and F. Merkt, The H_2^+ + HD reaction at low collision energies: H_3^+/H_2D^+ branching ratio and product-kinetic-energy distributions, Phys. Chem. Chem. Phys. **23**, 2676 (2021).

[34] L. Neale and J. Tennyson, A High-Temperature Partition Function for H_3^+, Astrophys. J. **454**, L169 (1995).

[35] I. Kylänpää and T. T. Rantala, First-principles simulation of molecular dissociation–recombination equilibrium, J. Chem. Phys. **135**, 104310 (2011).

[36] A. Znotins, F. Grussie, A. Wolf, X. Urbain, and H. Kreckel, An approach for multi-color action spectroscopy of highly excited states of H_3^+, J. Mol. Spectr. **378**, 111476 (2021).

[37] H. Kreckel, S. Krohn, L. Lammich, M. Lange, J. Levin, M. Scheffel, D. Schwalm, J. Tennyson, Z. Vager, R. Wester, A. Wolf, and D. Zajfman, Vibrational and rotational cooling of H_3^+, Phys. Rev. A **66**, 052509 (2002).

[38] R. Bejjani, A. Roucou, X. Urbain, K. Moshkunov, G. Vanlancker, and C. Lauzin, STARGATE: A new instrument for high-resolution photodissociation spectroscopy of cold ionic species, Rev. Sci. Instrum. **92**, 033307 (2021).

[39] H. Kreckel, H. Bruhns, K. A. Miller, E. Wâhlin, A. Davis, S. Höckh, and D. W. Savin, A simple double-focusing electrostatic ion beam deflector, Rev. Sci. Instrum. **81**, 063304 (2010).

[40] T. F. Thomas, F. Dale, and J. F. Paulson, Photodissociation of positive ions. I. Photodissociation spectra of D_2^+, HD^+, and N_2O^+, J. Chem. Phys. **67**, 793 (1977).

[41] R. G. Orth and R. C. Dunbar, Photodissociation of nitrous oxide cation, J. Chem. Phys. **66**, 1616 (1977).

[42] D. Klapstein and J. P. Maier, Lifetimes of $N_2O^+(A^2\Sigma^+)$ and $COS^+(A^2\Pi)$ in selected vibronic levels, Chem. Phys. Lett. **83**, 590 (1981).

[43] R. Frey, R. Kakoschke, and E. Schlag, Spectroscopy of molecular ions: Laser-induced fragmentation spectra of N_2O^+, $A^2\Sigma^+$-$X^2\Pi$, Chem. Phys. Lett. **93**, 227 (1982).

[44] S. Abed, M. Broyer, M. Carré, M. Gaillard, and M. Larzilliére, High-resolution spectroscopy of N_2O^+ in the near ultraviolet using fiblas (fast-ion-beam laser spectroscopy), Chem. Phys. **74**, 97 (1983).

[45] M. Larzillière, S. Abed, M. Carré, M. Gaillard, J. Lermé, and M. Broyer, l-Type doubling hyperfine structure of N_2O^+, Chem. Phys. Lett. **119**, 55 (1985).

[46] M. Larzillière and C. Jungen, Fast ion beam laser spectroscopy of N_2O^+, Mol. Phys. **67**, 807 (1989).

[47] H. Xu, Y. Guo, Q. Li, S. Liu, X. Ma, J. Liang, and H. Li, Spectroscopic study of $N_2O^+(A^2\Sigma^+)$ by photofragment excitation spectrum, J. Chem. Phys. **119**, 11609 (2003).

[48] A. Hirota, R. Igosawa, N. Kimura, S. Kuma, K. C. Chartkunchand, P. M. Mishra, M. Lindley, T. Yamaguchi, Y. Nakano, and T. Azuma, Radiative cooling dynamics of isolated N_2O^+ ions in a cryogenic electrostatic ion storage ring, Phys. Rev. A **102**, 023119 (2020).

[49] C. M. Western, PGOPHER: A program for simulating rotational, vibrational and electronic spectra, J. Quant. Spectrosc. Radiat. Transf. **186**, 221 (2017).